Epoxy Steel Slag Asphalt Mixture: Achieving Breakthrough in Pavement Performance and Efficient Waste Resource Utilization

Jia Sun [a], Wei Huang [b], Xinming Wang [c], Bohao Zhang [a, f], Zhihan Zhang [a], Ali Rahman [d], Yue Huang [e], Sang Luo [b*]

[a] *School of Transportation, Southeast University, Nanjing, Jiangsu, 211189, P. R. China*

[b] *Intelligent Transportation System Research Center, Southeast University, Nanjing, Jiangsu, 211189, P. R. China*

[c] *Suzhou Transport Investment Co., Ltd., Suzhou, Jiangsu, 215000, P. R. China*

[d] *School of Civil Engineering, University of Leeds, Leeds, LS2 9LG, UK*

[e] *Institute for Transport Studies, University of Leeds, Leeds, LS2 9JT, UK*

[f] *Nanjing Modern Multimodal Transportation Laboratory, Nanjing, Jiangsu, 211100, P. R. China*

*** To whom all correspondence should be addressed.**

Name: Prof. Sang Luo

Contact address: Intelligent Transportation System Research Center, Southeast University, Nanjing, Jiangsu, 210096, P. R. China

Tel/Fax: +86-13301586366

E-mail: 101011363@seu.edu.cn

Abstract: To address the key technical challenges of poor volume stability and insufficient moisture resistance that hinder the large-scale application of steel slag asphalt mixtures (SSAM), an innovative approach was proposed by incorporating epoxy asphalt (EA) into SSAM (EASSAM). Through a systematic investigation that entirely omitted the pretreatment of steel slag (SS), the effects of epoxy system (ES) content and SS replacement ratio on mixture performance were thoroughly examined, and the enhancement mechanisms were revealed through microstructural characterization. Meanwhile, a life cycle assessment was conducted to quantitatively evaluate the economic and environmental benefits of EASSAM. The results showed that increasing the ES content improved both the pavement performance and the long-term volume stability of EASSAM. The mixture with 20 wt% ES and 100% replacement of natural coarse aggregates with SS (EA20SS100AM) demonstrated outstanding comprehensive performance and was recommended for summer construction to accelerate traffic opening. ES effectively infiltrated the porous surface of SS, forming a dense coating layer and enhancing the adhesion between asphalt and aggregates, thereby effectively inhibiting performance deterioration and heavy metal leaching caused by moisture intrusion. Over the life cycle, EA20SS100AM achieved a 19.5% reduction in annualized costs and a 42.1% decrease in carbon emissions compared to commonly used SBS-modified asphalt mixtures. These research outcomes offer a practical technical solution for the large-scale utilization of SS resources while supporting reductions in natural aggregate extraction and promoting sustainable transportation infrastructure development with significant environmental, economic, and social benefits.

Keywords: Epoxy asphalt; steel slag asphalt mixture; pavement performance; improvement mechanism; sustainable development; benefit analysis

1. Introduction

With the continuous growth of the global economy, both production and demand for crude steel show a year-on-year increasing trend. In recent years, global annual crude steel production has consistently exceeded 1.8 billion tons. As the largest crude steel producer worldwide, China maintains annual output at approximately 1 billion metric tons, representing over 50% of total global production [1, 2]. As an inevitable byproduct of steelmaking processes, the stockpiling volume of steel slag (SS) continues to rise dramatically [3, 4]. However, the current comprehensive utilization rate of SS in China remains below 30% [5], significantly lower than that of developed countries (e.g., EU>90%, Japan>95%). This situation has led to massive open-air stockpiling of SS, causing severe environmental concerns. The inefficient utilization of SS not only constitutes resource waste but also poses multiple environmental risks through long-term accumulation. On one hand, it occupies substantial land resources and generates dust pollution; on the other hand, heavy metal elements (e.g., Cr^{6+}, Pb, Cd) in SS may migrate to surrounding soil and water systems through rainwater leaching [6]. Such a massive pollution scale exhibits long-term cumulative effects and poses potential hazards to both ecological systems and human health. Consequently, improving the resource utilization rate of SS is a critical issue that demands urgent resolution for sustainable development.

To address the environmental challenges posed by SS stockpiling, researchers have explored various reuse technologies by applying SS in fields such as construction materials, wastewater treatment, soil remediation, and catalyst development [7-9]. However, the applications in these fields have limited impact on the rapid consumption of SS. Against the backdrop of rapid urbanization, road construction offers significant opportunities for large-scale SS utilization. Currently, over 90% of roads in China are paved with asphalt pavement, the construction, operation, and maintenance of which require massive amounts of natural raw materials. Conventional aggregates are typically obtained through mountain blasting and quarrying [10], a process that generates substantial greenhouse gas emissions and causes severe ecological damage, and contradicts sustainable development principles [11]. In comparison, effective SS recycling can not only reduce environmental pollution from heavy metal leaching but also decrease dependency on natural raw materials and aggregates. Overall, the application of SS in asphalt pavement construction contributes to ecological conservation and promotes sustainable infrastructure development.

Despite demonstrating certain advantages in pavement engineering applications, the large-scale implementation of SS still faces critical technical challenges. Early research have indicated that SS possesses excellent wear resistance, angularity, and hardness. When mixed with other aggregates, SS can create an embedding effect that enhances the strength of asphalt mixtures while reducing pavement costs [12-14]. Some scholars have attempted to use aged SS as a 100% replacement for limestone coarse aggregate and conducted preliminary studies on its pavement performance. Although test results demonstrated improved mechanical properties of the asphalt mixture, critical analyses of long-term volume stability and moisture damage resistance were lacking [15, 16]. The free oxides in SS readily undergo hydration reactions with moisture, leading to pavement defects such as rust moisture seepage, network cracking, and localized upheaval, which compromise the durability of the pavement [17]. Consequently, improving the volume stability of SS, minimizing application-induced defects, and achieving efficient SS reuse in pavement engineering have become key research focuses. To address these challenges, researchers have conducted systematic optimization studies on the volume stability and anti-stripping performance of SSAM. Results indicate that natural aging provides only a limited improvement to the volume stability of the SSAM, and long-term storage of SS asphalt mixtures contributes to dust pollution, additional carbon emissions, and land occupation[18, 19]. Some researchers have employed surface modifiers to pretreat SS, finding that enhanced interfacial strength between SS and asphalt can improve SSAM performance [20, 21]. Notably, despite extensive research on SSAM performance optimization and design, pretreatment processes remain complex with limited performance enhancement, and the desirable substitution rate of SS for natural aggregates in asphalt mixtures has yet to exceed 50%. The primary reasons for the poor moisture resistance of SSAM are adhesive failure between asphalt and aggregates and loss of asphalt cohesion [22]. If the binder cannot effectively coat SS, moisture rapidly deteriorates the bonding performance of SSAM, ultimately leading to stripping and rusting issues. Surface treatment alone cannot fully prevent SSAM bonding failure or ensure mixture durability [23]. Therefore, exploring high-performance asphalt materials for SSAM applications has emerged as a critical direction for overcoming these technical barriers.

Epoxy asphalt (EA) represents a high-performance asphalt material wherein the epoxy resin and curing agent undergo crosslinking reactions upon mixing. The resulting three-dimensional network structure effectively restricts asphalt molecular migration while simultaneously enhancing both asphalt-aggregate adhesion and intrinsic cohesive strength [24, 25]. Extensive research confirms that epoxy asphalt mixtures (EAM) demonstrate superior comprehensive pavement performance, particularly regarding high-temperature stability and moisture resistance, with current applications predominantly in orthotropic steel bridge decks and airport pavements [26-29]. Given these demonstrated engineering advantages, EA shows significant potential as a high-performance material for conventional road construction. The optimal mass ratio of epoxy system (ES) in EA typically reaches 50 wt% to ensure the formation of a continuous phase-network structure within the asphalt matrix [30]. However, the relatively lower performance requirements of highway pavements compared to specialized applications, combined with the substantial cost implications of high ES content, have limited the widespread adoption of EAM in general road engineering. Recent investigations into reduced-epoxy formulations reveal that even a diminished resin content can substantially enhance pavement performance while significantly lowering construction costs [31, 32]. From a life cycle assessment perspective, EAM qualifies as a long-life pavement material with dramatically reduced maintenance needs, leading to advantages in both energy consumption and carbon emissions throughout its service life [33].

In summary, this study aims to apply EA to SSAM by leveraging its high-performance characteristics to overcome the critical technical challenges of long-term volume instability and poor moisture resistance in SSAM while completely eliminating the complex pretreatment processes traditionally required for SS, ultimately achieving 100% replacement of natural coarse aggregates with SS. This innovative approach not only significantly alleviates land occupation and environmental pollution risks caused by SS stockpiling but also reduces natural aggregate extraction through a "waste-for-virgin-materials" model, thereby advancing transportation infrastructure toward net-zero carbon emissions. To this end, the study prepared epoxy steel slag asphalt mixture (EASSAM), systematically investigated the evolution of pavement performance under varying ES contents and SS replacement ratios, and employed microscopic testing to analyze the enhancement mechanisms of ES in the mixture. Furthermore, the economic and environmental advantages of EASSAM were quantitatively analyzed using life cycle assessment and leaching tests. The research outcomes hold positive implications for reducing environmental burdens and promoting sustainable development in transportation infrastructure.

2. Materials and Design

2.1. Raw Materials

This study utilized matrix asphalt (Jinling Petrochemical Co. Ltd., China), a self-developed EB2-EAA10 epoxy resin system based on E51 bisphenol A epoxy resin and amine curing agent, SS (Jiangsu Yonggang Group Co. Ltd., China), basalt aggregate (BA), and mineral powder (Zhenjiang Changfeng Building Materials Co. Ltd., China) as the primary materials for asphalt mixture preparation, part of the raw material is shown in Fig. 1. The matrix asphalt, epoxy resin, curing agent, ES, and EA were tested according to "Standard Test Methods of Bitumen and Bituminous Mixtures for Highway Engineering" (JTG E20-2011), "Plastics - Determination of tensile properties" (GB/T 1040.1-2018), "Plastics—Epoxy Compounds—Determination of Epoxy Equivalent" (GB/T 4612-2008), and "Plastics—Amine Epoxide Hardeners—Determination of Primary, Secondary and Tertiary Amine Group Nitrogen Content" (ISO 9702:1996) [34-37], with their basic properties shown in Table 1. Coarse SS serves as an ideal substitute for natural aggregates in asphalt mixtures. This is because, compared to coarse SS, fine SS (＜4.75 mm) possesses a substantially larger specific surface area, resulting in a significantly higher risk of volume expansion upon moisture exposure. Consequently, fine SS is typically employed in applications such as 3D printing and soil remediation [9, 19, 38]. This study utilized freshly produced, untreated basic oxygen furnace (BOF) molten slag, which was sieved into two size fractions: 9.5-16 mm and 4.75-9.5 mm. X-ray fluorescence (XRF) spectroscopy was performed on both SS and BA, with results presented in Table 2. The analysis reveals that CaO, Fe_2O_3, and MgO collectively account for 68.01% of SS composition, while BA primarily consists of SiO_2 and Al_2O_3. The X-ray diffraction (XRD) test results of SS and BA can be found in the previous study [21]. The SS primarily consists of $(CaO)_2 \cdot Fe_2O_3$, $(CaO)_3 \cdot SiO_2$, $(CaO)_2 \cdot SiO_2$, CaO, calcium silicate hydrate (C-S-H), and divalent metal oxide continuous solid solution (RO phase). In contrast, the main components of BA are $Na(AlSi_3O_8)$, $Ca(AlSi_3O_8)$, $Ca(Fe,Mg)Si_2O_6$, and SiO_2. All aggregate properties complied with Chinese standards "Test Methods of Aggregate for Highway Engineering"

(JTG E42-2024) and "Steel Slag for Road" (GB/T 25824-2010) [39, 40], with their technical specifications presented in Table 3.

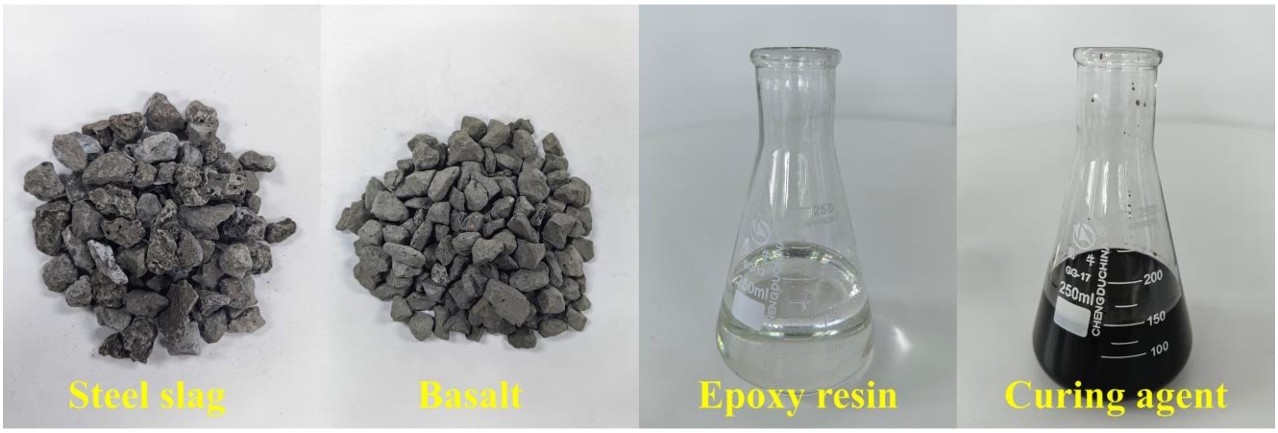

Fig. 1. Raw materials

Table 1. Basic properties of matrix asphalt, epoxy resin, curing agent, ES, and EA

Material type	Basic property
Matrix asphalt	Penetration (25°C, 100g, 5s): 64.2 (0.1mm); Softening Point (TR&B): 47.2°C; Ductility (10°C, 5cm/min): 20.6 cm; Dynamic viscosity (60°C): 203.9 Pa·s; Density (25°C): 1.018 g/cm^3
Epoxy resin	Viscosity (23°C): 16,000 mPa·s; Epoxide equivalent: 195 g/eq; Density (25°C): 1.083 g/cm^3; Exterior condition: Light yellow transparent liquid.
Curing agent	Amine value: 189 mgKOH/g; Density (25°C): 0.841 g/cm^3; Exterior condition: Black liquid.
ES	Tensile strength (23°C): 7.8 MPa; Elongation at break (23°C): 163.7%
Epoxy Asphalt (with 40 wt% ES content)	Tensile strength (23°C): 3.9 MPa; Elongation at break (23°C): 271.6%

Table 2. XRF test results for different aggregates

Aggregate type	Content/%								
	CaO	Fe_2O_3	SiO_2	Al_2O_3	MnO	MgO	P_2O_5	Cr_2O_3	other
BA	8.76	10.84	44.94	17.08	0.16	4.61	0.60	0.08	12.93
SS	40.00	22.20	15.38	6.01	5.06	6.01	2.89	0.50	1.95

Table 3. Technical specifications of aggregates

Indicator		Unit	SS	BA
Apparent density	9.5-16mm	g/cm^3	3.476	2.947
	4.75-9.5mm		3.451	2.941
	2.36-4.75mm		/	2.934
	0-2.36mm		/	2.801
Water absorption	9.5-16mm	g/cm^3	1.713	1.179
	4.75-9.5mm		1.832	1.386
	2.36-4.75mm		/	1.421
	0-2.36mm		/	1.512
Crushing value		%	14.4	11.1
Los Angeles Wear Value		%	14.2	12.1
Content of needle and flake particles		%	8.9	7.6
Washing method <0.075mm particle content		%	0.41	0.55
Grinding value		/	44	52

2.2. Mixture Preparation

In special pavement applications such as orthotropic steel bridge decks, the ES content in EA typically reaches as high as 50 wt%, resulting in significantly increased material costs [41]. Previous studies have indicated that highway pavements experience lower traffic volume and loading compared to specialized pavements. By appropriately reducing the ES content in EA while meeting performance requirements, a balance can be achieved between pavement performance and economic feasibility [31, 42]. Therefore, this study employed EA with ES contents of 10, 15, and 20 wt%, designated as EA10, EA15, and EA20 respectively.

As shown in Table 3, the density of SS is approximately 15% higher than that of BA. Consequently, it was necessary to convert the mass ratio to volume ratio based on aggregate densities to minimize gradation differences in the mixtures caused by density variations [5]. To analyze the effect of SS replacement level on mixture performance, this study prepared asphalt mixtures with 0, 50, and 100 vol% SS replacement of BA coarse aggregate were prepared. These mixtures were labeled as SS0AM, SS50AM, and SS100AM respectively.

The preparation process of EA involved the following steps: i) preheating the matrix asphalt and EB2-EAA10 system to 160°C and 60°C respectively; ii) mixing the EB2 and EAA10 at a mass ratio of 60:40 followed by stirring at 60°C for 3 min to obtain ES; iii) blending ES with matrix asphalt at 160°C for 4 min to produce EA.

The preparation process of the mixture was optimized based on previous research findings [5, 21]. The specific preparation procedure consisted of: i) preheating matrix asphalt and aggregates (including BA and SS) to 160°C and 185°C respectively; ii) setting the mixer temperature to 170°C, adding aggregates, and mixing for 60 s at 170°C; iii) incorporating the prepared EA into the mixer and maintaining mixing for the same duration; iv) adding mineral powder and continuing mixing for 60 s to obtain the final mixture for specimen molding.

2.3. Mixture gradation design

This study adopted the AC-13 gradation, commonly used for pavement surface layers, for mixture design. Previous studies have demonstrated that the ES content in EA does not significantly affect the optimal asphalt-aggregate ratio of asphalt mixtures [24, 43]. In contrast, SS possesses high porosity and a rough surface texture, requiring additional asphalt to achieve complete coating. Therefore, it is necessary to determine the optimal asphalt-aggregate ratio for different SSAMs. Based on prior research, gradation design for various mixture compositions was completed using the volume replacement method [5, 21], with results presented in Fig. 2. In accordance with Chinese standard (JTG E20-2011) [34], SSAM specimens were prepared using EA20 to investigate the optimal asphalt-aggregate ratio for mixtures with varying SS replacement rates. The final optimal asphalt-aggregate ratios were established as 5.1% for SS0AM, 5.4% for SS50AM, and 5.8% for SS100AM. For analytical clarity, a systematic nomenclature was developed for all asphalt mixtures, as illustrated in Fig. 3.

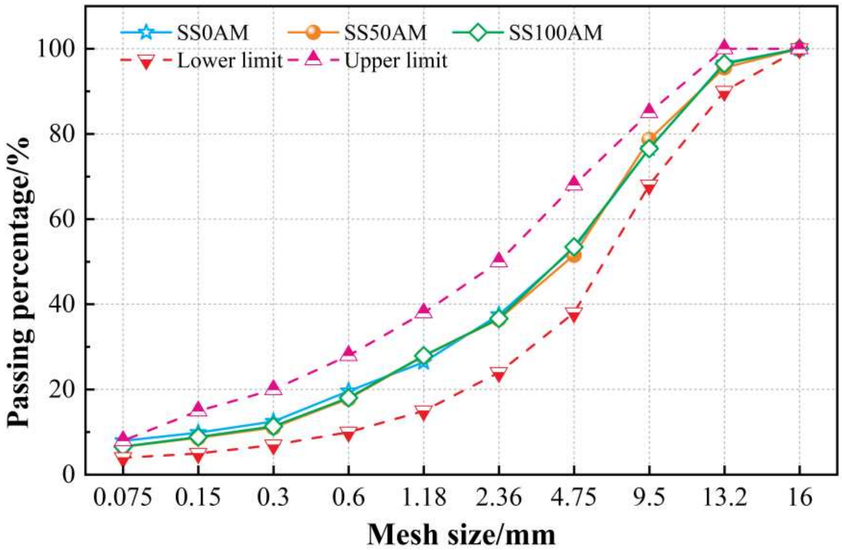

Fig. 2. Gradation design results

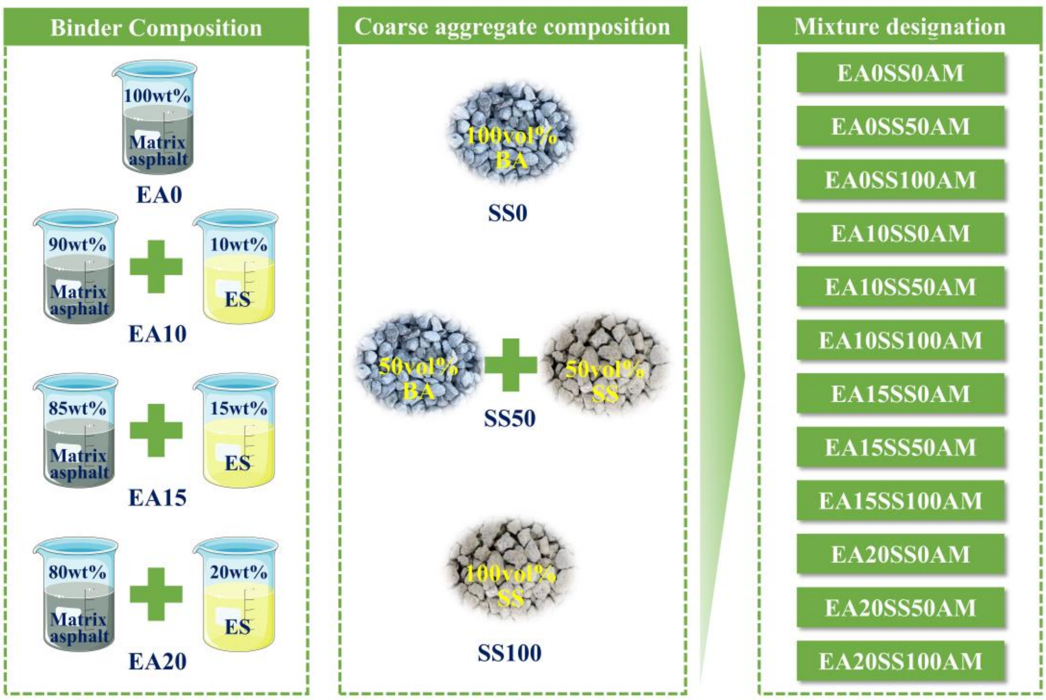

Fig. 3. Designation of different mixtures

3. Test Methods

3.1. Pavement performance test

According to Chinese standards (JTG E20-2011) [34], specifically T0709-2011, T0729-2000, T0719-2011, and T0715-2011, a series of tests, including the immersion Marshall test, freeze-thaw splitting test, rutting test, and beam bending test, were conducted to analyze and compare the moisture stability, high-temperature rutting resistance, and low-temperature cracking resistance of asphalt mixtures with different ES and SS contents. It should be noted that all tests were performed using three parallel specimens.

In the immersion Marshall test, the standard Marshall specimens were divided into two groups: one group was stored at room temperature as the control, while the other group was subjected to immersion in a constant-temperature water bath under conditions of 60°C for 48 h. Subsequently, both groups of specimens were placed in a 60°C water bath for 30 min to reach temperature equilibrium. The *MS* of each specimen was then measured using a Marshall testing machine. Finally, the Residual Stability (*RS*) was calculated to evaluate the moisture damage resistance of the asphalt mixture.

For the freeze-thaw splitting test, two groups of standard Marshall specimens were prepared and subjected to vacuum saturation treatment. One group underwent a complete freeze-thaw cycle consisting of 16 h freezing at -18°C followed by 24 h immersion in a 60°C water bath, while the other group was maintained at room temperature as the control. Subsequently, both groups of specimens were immersed in a 25°C water bath for 2 h to achieve temperature equilibrium. The splitting strength of each specimen was then determined using the splitting test attachment of the Marshall testing machine. Finally, the Splitting Strength Ratio (*SSR*) was calculated to evaluate the freeze-thaw resistance of the asphalt mixture.

In the rutting test, slab specimens (300×300×50 mm) were prepared using the roller compaction method. Before testing, the specimens were conditioned at 60°C for 4 h to achieve temperature equilibrium. The specimens were then placed in the rutting tester, where a loaded wheel passed over them at a speed of 42 times/min under controlled conditions of 60°C for 60 min. Finally, the dynamic stability (*DS*) was calculated based on the deformation measured at 45 and 60 min to evaluate the high-temperature rutting resistance of the asphalt mixture.

For the beam bending test, the slab specimens were cut into beam specimens (250×30×35 mm). Before testing, the specimens were placed in a constant temperature chamber at -10°C for 4 h. Then, the servo-hydraulic multi-functional universal testing machine (UTM)-25 was used to conduct three-point bending loading on the specimens until failure. The test was performed at a rate of 50 mm/min and a temperature of -10°C. Finally, the maximum load at failure and the mid-span deflection were recorded to calculate the flexural tensile strength (*RB*) and maximum flexural strain (ε_B), thereby evaluating the low-temperature cracking resistance of the asphalt mixture.

Additionally, according to T0739-2011 of the Chinese standard (JTG E20-2011) [34], the four-point bending fatigue test was conducted to evaluate the fatigue resistance of asphalt mixtures for life cycle assessment analysis. Beam specimens measuring 380×50×63.5 mm were prepared and tested using a UTM-130 servo-hydraulic multifunctional material testing system. The tests were performed under temperature conditions of 15±0.5°C, employing strain-controlled mode (10 Hz sinusoidal wave) at a strain level of 400 με. Notably, the fatigue life (N_f) was determined as the number of loading cycles when the modulus degraded to 50% of its initial value.

3.2. Long-term volume stability test

The main reason for SS has not been widely used in pavement engineering is its water-induced expansion tendency, which can cause pavement defects like cracking and spalling. Therefore, this study focuses on evaluating the long-term volume stability of asphalt mixtures with different ES and SS contents. It should be noted that there is currently no standard test procedure for assessing the volume stability of asphalt mixtures. Based on relevant literature and preliminary exploratory tests [44], volume stability was evaluated by measuring the volume changes of Marshall specimens under high-temperature water immersion. Previous studies have tested the long-term moisture stability of SSAM and found that after 10 d of immersion, significant stripping occurred on the surface of the mixture, and the moisture stability could no longer meet the specification requirements [21]. Given the excellent performance of EA, the asphalt film formed on the aggregate surface is not easily damaged, which may reduce moisture intrusion and thereby significantly improve the long-term volume stability of SSAM. For this reason, this study set the high-temperature immersion duration to a sufficiently long period of 60 d. First, six points were marked at 60° intervals on the surface of Marshall specimens, and a vernier caliper was used to measure six height values and three diameter values at the marked positions, with averages calculated. Then, the specimens were immersed in a 60°C water bath, and their height and diameter at the marked positions were measured every 3 d, with a total immersion duration of 60 d. The volume expansion ratio (*P*) was calculated as shown in Eq. (1):

$$P_{\mathrm{i}}=\frac{V_{\mathrm{i}}-V_0}{V_0} \tag{1}$$

where P_{i} is the expansion rate of the specimen on the *i* d, %; V_{i} is the volume of the specimen after *i* d soaking, cm^3; V_0 is the Volume of the unsoaked specimen.

3.3. Marshall test

Standard Marshall specimens (Φ101.6×63.5 mm) were prepared according to the T0702-2011 in Chinese standard (JTG E20-2011) [34], with 75 blows of compaction on each side. After curing the specimens in an oven at 60°C, the Marshall stability (*MS*) of the specimens was tested using a Marshall testing machine. The curing degree (ω) was employed to evaluate the influence of temperature on the curing progress, with the calculation as shown in Eq. (2).

$$\omega=\frac{MS_{\mathrm{i}}\text{-}MS_0}{MS_4\text{-}MS_0} \quad (2)$$

where ω is the curing degree of the asphalt mixture, %; MS_{i} is the Marshall stability of specimen at i d of curing, kN; MS_0 is the Marshall stability of the uncured specimen, kN; MS_4 is the Marshall stability at 60°C/4 d of curing, kN.

3.4. LSCM test

The microscopic distribution of the ES phase (green areas) and asphalt phase (black areas) in EA was observed using laser scanning confocal microscopy (LSCM) (Leica TCS SP8, Germany) under 488nm Ar^+ laser excitation. Prepared EA10, EA15, and EA20 samples were applied onto glass slides using a glass rod, covered with coverslips, and cured in a 60°C oven for 4 d before LSCM testing. Observations were conducted at 40× magnification.

3.5. SEM test

The microscopic morphology of interfaces between different aggregates (BA and SS) and asphalt binders (matrix asphalt and EA20) was investigated using an FEI Inspect F50 scanning electron microscope (SEM) (ThermoFisher, USA). The aggregate-asphalt interface samples were prepared as follows: first, SS and BA were separately immersed in matrix asphalt and EA at 160°C using tweezers, allowing the asphalt to adhere to half of the surface of each aggregate. The samples were then placed in a 150°C oven for 2 h to ensure complete asphalt flow and removal of excess binder while promoting thorough wetting of the aggregate surfaces. The prepared specimens were designated as EA0-BA, EA0-SS, EA20-BA, and EA20-SS according to their respective interface combinations. Before testing, the samples were gold-coated to enhance conductivity and achieve optimal imaging quality. The test was conducted using an Everhart-Thornley detector with an electron acceleration voltage of 20.0 kV, at magnifications of 300× and 5000× respectively.

3.6. Leaching test

In accordance with the Chinese standard "Identification standards for hazardous wastes—Identification for extraction toxicity" (GB5085.3-2007) [45], the concentrations of cadmium (Cd), hexavalent chromium (Cr^{6+}), lead (Pb), mercury (Hg), and arsenic (As) in the leachates of SS and EA20SS100AM were tested using a SPECTROBLUE inductively coupled plasma optical emission spectrometer (ICP-OES). The leachate of SS was prepared following the Chinese standard "Solid waste-Extraction procedure for leaching toxicity-Sulphuric acid & nitric acid method" (HJ/T 299-2007) [46]. For EA20SS100AM, an improved leaching method proposed in previous studies was adopted. Specifically, standard Marshall specimens were immersed in a mixture of distilled water and acetic acid maintained at 60°C in a constant-temperature water bath for 10 d to thoroughly simulate the effects of high temperatures and precipitation during pavement service. It should be noted that water and acetic acid were replenished every 12 h to maintain the pH at 5.0 ± 0.2 [21].

4. Results and discussion

4.1. Pavement performance

4.1.1. Moisture stability

The moisture stability test results appeared in Fig. 4. The immersion Marshall test revealed that under identical ES content conditions, SS50AM demonstrated the highest *MS* value, followed by SS100AM, while SS0AM showed the weakest performance. This phenomenon suggested that proper SS incorporation could form a more stable skeleton interlocking structure, significantly enhancing the mechanical strength of the mixture [47]. Meanwhile, increasing ES content produced positive effects on EASSAM performance. Specifically, EA20SS50AM reached an *MS* value of 49.2 kN, representing a 270% improvement compared with EA0SS50AM. Mixtures utilizing matrix asphalt and EA10 failed to satisfy the specification requirement (JTG F40-2004) of *RS*≥85% [48]. Notably, in mixtures prepared with matrix asphalt, increasing the SS replacement ratio led to *RS* decline, indicating matrix asphalt could not alleviate the volume stability reduction caused by higher SS content, resulting in progressively deteriorating moisture stability. In contrast, when employing EA15 and EA20, elevating the SS replacement ratio markedly improved the water resistance and strength of the mixture. Specifically, the *RS* of the EA20SS100AM achieved 94.6%, showing 15.7% and 4.1% improvements over EA0SS100AM and EA20SS0AM, respectively. The results indicated that while complete SS replacement of BA coarse aggregates caused slight *MS* reduction, ES incorporation could significantly enhance water damage resistance of SS-containing asphalt mixtures, with moisture stability improving progressively as ES content increased.

The freeze-thaw splitting test results appeared in Fig. 4(c) and (d). Under identical ES content conditions, SS50AM demonstrated superior splitting strength compared to SS0AM and SS100AM. Meanwhile, with increasing ES content, the splitting strength of mixtures showed an ascending trend, with EA20SS50AM reaching the peak value of 2.15 MPa, representing a 172% improvement compared to EA0SS100AM (0.79 MPa). This pattern exhibited good consistency with the immersion Marshall test results. From the perspective of freeze-thaw sensitivity, mixtures prepared with matrix asphalt showed gradually decreasing *SSR* as SS content increased, indicating that SS addition negatively affected water stability, which constituted the main reason for investigating the applicability of EA in SSAM. With ES incorporation, mixtures with identical SS content demonstrated increasing *SSR*. However, for SSAM prepared with EA10 and EA15, excessive SS addition tended to cause *SSR* reduction. In contrast, when applying EA20 in SSAM, *SSR* continued to rise with increasing SS content. Specifically, EA20SS100AM achieved 93.2% of *SSR*, significantly exceeding the requirement (≥75%) in the specification (JTG F40-2004) and showing a 13.0% improvement over EA0SS100AM [48]. Notably, during splitting tests, specimens underwent uniaxial lateral force, where the bonding performance at the asphalt-aggregate interface played a dominant role [49]. The results indicated that the excellent bonding properties of EA20 enhanced adhesion between aggregate and asphalt, while the strong bonding at the SS-EA interface effectively blocked moisture intrusion, minimizing internal stress damage caused by freeze-thaw cycles.

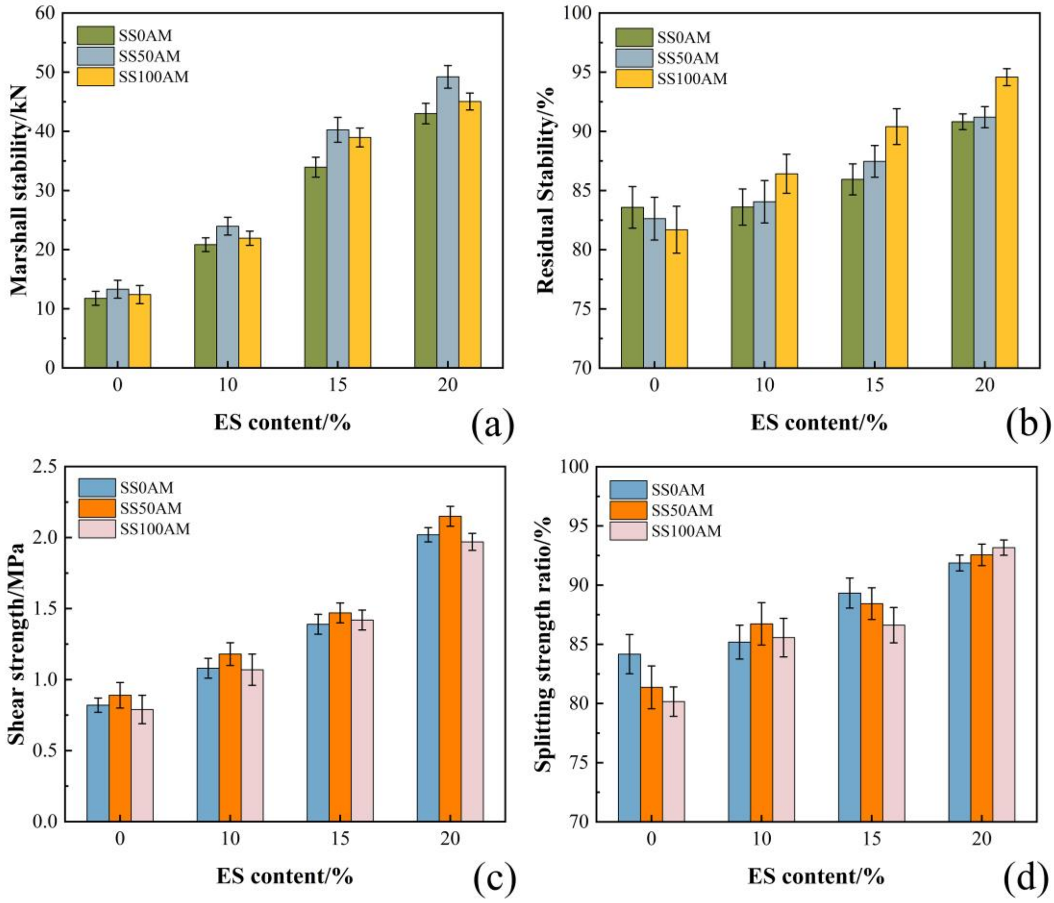

Fig. 4. Moisture stability test results:

(a), (b) water immersion Marshall test; (c), (d) freeze-thaw splitting test

4.1.2. Rutting resistance

The rutting test results appear in Fig. 5. In mixtures prepared with matrix asphalt, the rut depth (*RD*) increased while *DS* decreased as the SS replacement ratio rose, indicating deterioration in rutting resistance performance. The *DS* value for EA0SS100AM measured only 2,157 times/mm, failing to meet the minimum requirement of 2,800 times/mm specified in JTG F40-2004 [48]. Furthermore, EA10 provided limited improvement to the high-temperature rutting resistance of SSAM. However, when ES content increased to 15% and 20%, the negative impact of SS on high-temperature rutting resistance gradually weakened, with all *DS* values exceeding 10,000 times/mm. Specifically, EA20SS50AM achieved a *DS* value of 20,322 times/mm, representing a 494% improvement compared with EA0SS50AM. During rutting tests, asphalt mixtures primarily endured vertical stress. Compared with BA, SS exhibited higher crushing values, resulting in relatively fragile skeleton structures and poor rutting resistance when no ES was added. The introduction of ES enhanced the viscosity properties between aggregate and asphalt, strengthening the overall shear resistance of the structure [50, 51]. Additionally, the porous characteristics of SS facilitated better coating of EA on aggregate surfaces, while chemical bonding at the EA-SS interface significantly improved adhesive strength, leading to remarkable enhancement of high-temperature rutting resistance. The results demonstrated that EA20SS100AM attained a *DS* value of 19,091 times/mm, which was slightly lower than EA20SS50AM but substantially higher than specification requirements, exhibiting excellent high-temperature stability.

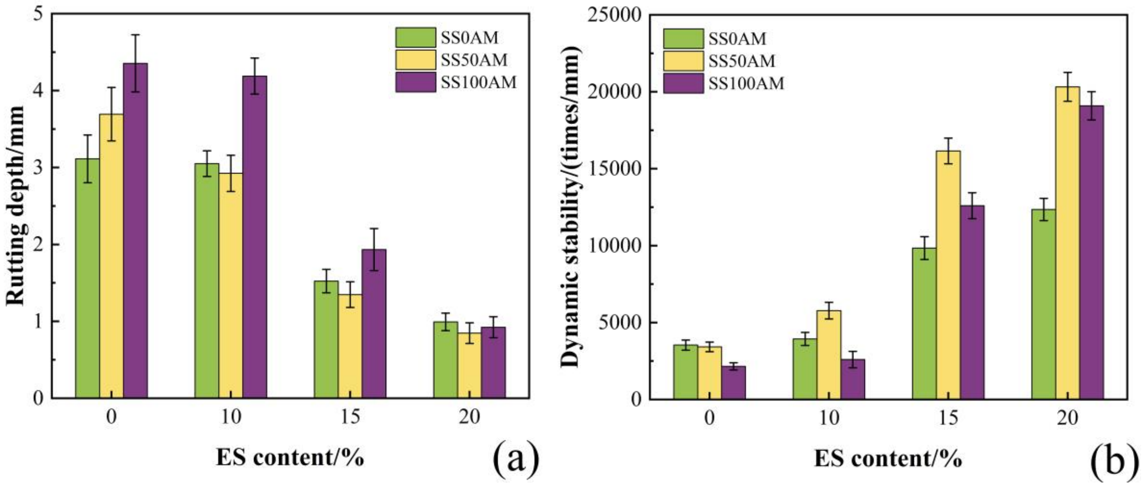

Fig. 5. Rutting test results: (a) *RD*; (b) *DS*

4.1.3. Cracking resistance

The beam bending test was conducted to evaluate the low-temperature performance of mixtures with different ES contents and SS replacement ratios, with results shown in Fig. 6. Under identical ES content conditions, both *RB* and ε_B of the mixtures gradually increased as the SS replacement ratio rose. Similarly, increasing ES content also improved the low-temperature performance. Among all mixtures, EA20SS100AM demonstrated optimal performance, achieving *RB* and ε_B values of 20.29 MPa and 2,249 με respectively. According to specification JTG F40-2004, the ε_B of high-modulus asphalt mixtures should not be less than 1,800 με [48]. The ε_B of EA20SS100AM showed 29.9% and 29.3% improvements compared with EA20SS0AM and EA0SS100AM respectively. Overall, the synergistic effect between ES and SS effectively enhanced the low-temperature performance of mixtures. On one hand, the porous and angular characteristics of SS provided a greater specific surface area which absorbed more asphalt, improving both the interlocking effect between aggregates and the adhesion between aggregate and asphalt [5, 21]. On the other hand, the low viscosity of ES endowed EA with good fluidity and permeability before curing, enabling the complete filling of voids in SS aggregates , thereby forming more uniform and dense mixture structures [30]. These factors collectively contributed to improved deformation capacity and crack resistance of mixtures under low-temperature conditions.

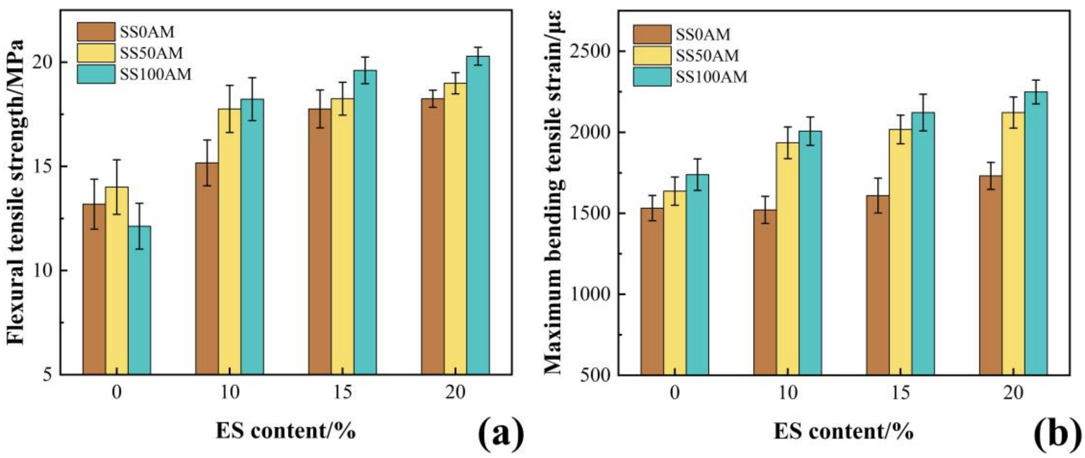

Fig. 6. Bending beam test results: (a) *RB*; (b) ε_B

4.2. Long-term volume stability

To simulate extreme high-temperature and moisture effects on pavement, the mixtures were subjected to 60°C/60 d immersion to evaluate volume stability, with test results shown in Fig. 7. It was found that using SS to replace natural aggregates significantly affected the volume stability of asphalt mixtures. Specifically, EA0SS100AM and EA0SS50AM reached *P* values of 2.91% and 2.57% after 9 and 15 d immersion respectively, far exceeding the 1.5% limit specified in GB/T 24175-2009, accompanied by surface distresses such as bulging and peeling [39]. The addition of ES caused P_{60} to decrease, with EA20SS50AM maintaining P_{60} below 1.5%. As ES content increased, the volume expansion rate of mixtures with the same SS content gradually decreased, and the late-stage growth increment progressively reduced. Notably, after 60 d immersion, mixtures prepared with EA20 eventually stabilized in *P* value, showing over 60% reduction compared with EA0SS50AM and EA0SS100AM. This improvement exceeded other surface treatment technologies reported by Gan et al. and Sun et al. [5, 52], which showed 34.2% and 13.9% improvements respectively. The results demonstrated that the three-dimensional crosslinked network formed by ES at asphalt-aggregate interfaces effectively inhibited moisture intrusion and SS expansion, while complete filling of SS porous structure by EA enhanced interfacial bonding. These mechanisms significantly delayed the water-induced expansion of SS, enabling the mixtures to meet stringent durability requirements for long-life pavement.

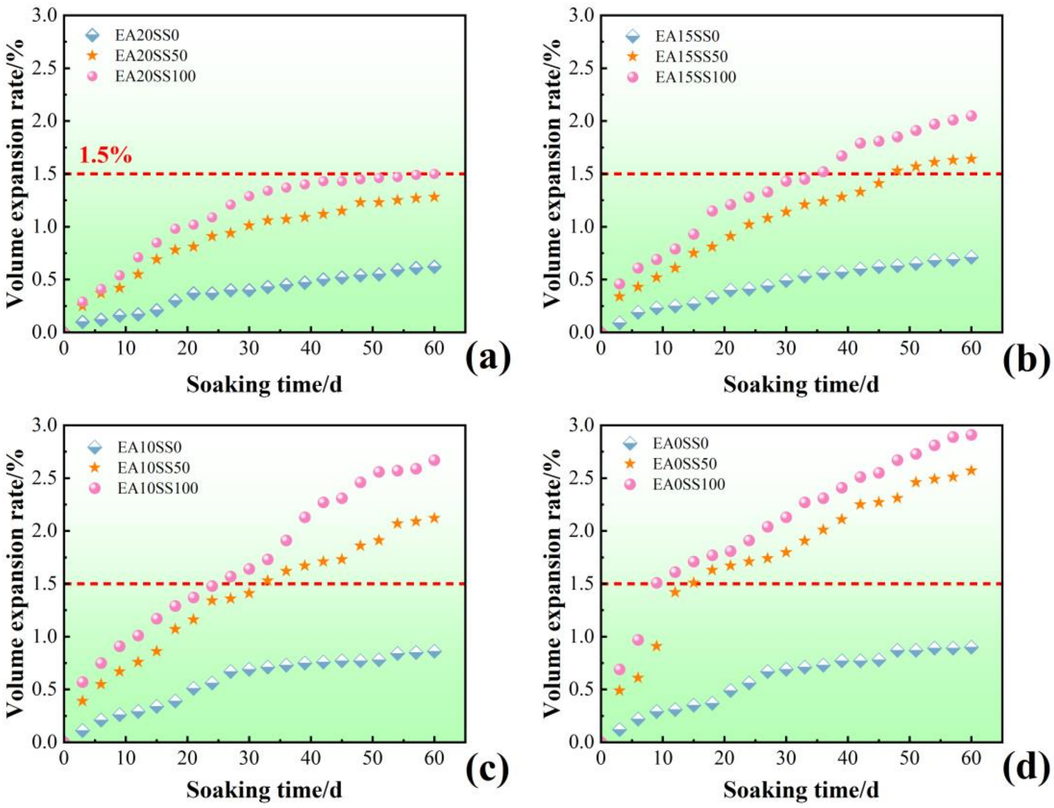

Fig. 7. Long-term volume stability test results:

(a) EA20SSAM; (b) EA15SSAM; (c) EA10SSAM; (d) EA0SSAM.

4.3. Effect of temperature on the curing process

As a typical thermosetting material, ES imparted pronounced curing time-temperature dependence to the *MS* of EA-based mixtures [31, 42]. Through testing *MS* under different curing conditions and calculating ω using Eq. (2), the influence of curing conditions on EASSAM performance underwent systematic analysis, with results displayed in Fig. 8. The standard curing condition for EB2-EAA10 system was 60°C/4 d, hence ω under this condition served as 100%. Fig. 8 revealed that after 1 day curing at 60°C, ω jumped sharply to 73.6%. When the curing duration reached 2 d, ω had attained 91.3%, showing near-completion of curing reactions within the system, aligning with previous research findings [31]. Subsequently, ω demonstrated a gradual increase with extended curing time, stabilizing after 4 d. By contrast, specimens cured at 40°C exhibited slower curing rates, reaching 85.6% of ω after 4 d and stabilizing after 10 d. Notably, curing at 20°C progressed extremely slowly - after 4 d curing, ω registered only 34.9%, requiring 20 and 25 d curing durations to exceed the curing levels achieved by 1 and 2 d at 60°C respectively, with the curing process not concluding until 35 d. Therefore, EASSAM proved most appropriate for summer construction to guarantee strength development and rapid traffic opening. For construction during other seasons, laboratory determination of strength development patterns became necessary, with a corresponding extension of traffic opening times.

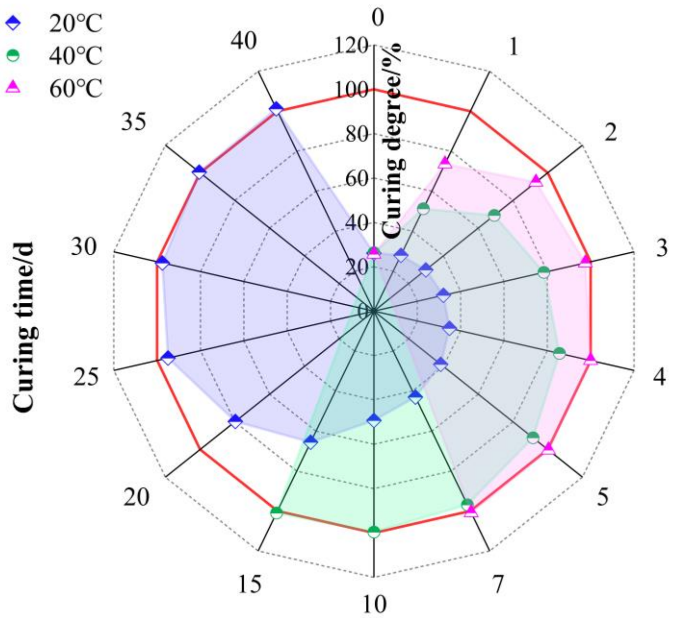

Fig. 8. Curing degree of mixtures at different curing conditions

4.4. Performance enhancement mechanism

4.4.1. Microscopic phase distribution

The LSCM results of EA with different ES contents after 4 d curing at 60°C are shown in Fig. 9. It was observed that the ES phase in EA10 appeared relatively sparse, while in EA15 and EA20, ES particle diameters significantly increased and aggregated into irregular large particles that uniformly dispersed within the asphalt phase, effectively hindering asphalt flow. Although no phase transition occurred in the EA, these ES particles could be distributed between the aggregate voids, thus significantly improving the overall adhesion. From an interfacial chemistry perspective, the hydroxyl-containing main chains in ES substantially enhanced EA viscosity [53] while highly reactive epoxy groups reacted with active hydrogen in both curing agents and asphalt, thereby improving the bonding capability and stability of the EA around aggregate surfaces [54, 55]. Consequently, compared to matrix asphalt and EA10, EA20 more effectively mitigated water-induced damage to aggregates, maintaining excellent volume stability and moisture stability even with 100% SS replacement of BA coarse aggregates.

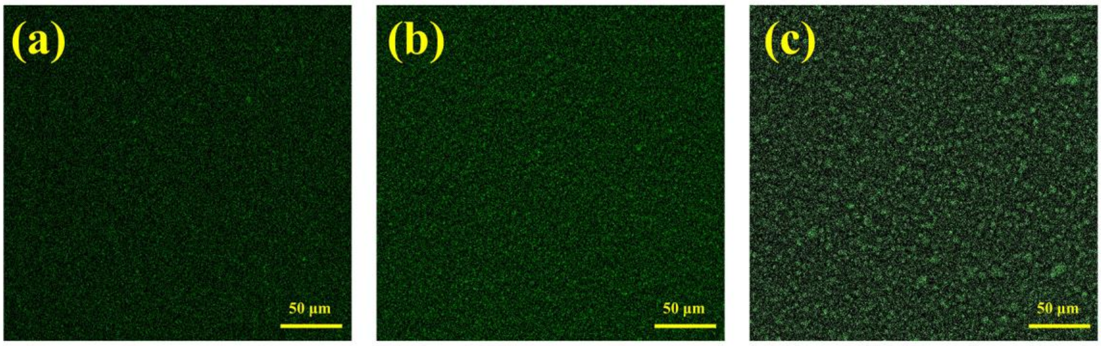

Fig. 9. Results of LSCM tests with different ES contents: (a) EA10, (b) EA15 (c) EA20

4.4.2. Aggregate-asphalt interface morphology

The microscopic surface morphology of BA, SS, and their interfaces with matrix asphalt and EA20 were observed using SEM, with results presented in Fig. 10. As shown in Fig. 10(a) and (d), BA exhibited smooth, continuous and uniform texture with minimal undulation. In contrast, SS displayed rough surfaces with numerous textures and pores. Additionally, abundant loose and irregularly shaped crystalline substances were attached to SS surfaces, primarily consisting of unreacted CaO, RO phase and CaO generated from C_3S decomposition [5, 56]. Fig. 10(c) and (f) revealed that EA20 uniformly distributed across the surface of SS and BA, indicating complete wetting and formation of dense coating layers on aggregate surfaces. Comparatively, as shown in Fig. 10(b) and (e), matrix asphalt exhibited significant peeling on both SS and BA surfaces, failing to achieve complete aggregate encapsulation. Under such conditions, moisture intrusion could easily cause asphalt film peeling, subsequently leading to volume expansion of SS and pavement distress. These phenomena were attributed to two factors. On one hand, the lower initial viscosity of EA20 facilitated the complete coating of SS surfaces; on the other hand, as an alkaline aggregate, SS contained Ca^{2+} that reacted with epoxy groups in EA to form Ca-O-C covalent bonds. Simultaneously, N-H groups in the amine-based curing agent interacted with Ca^{2+} to produce Ca-N bonds, which enhanced the interfacial adhesion between asphalt and aggregate [57]. SEM results further confirmed the superiority and feasibility of EA application in SSAM at the microscopic level.

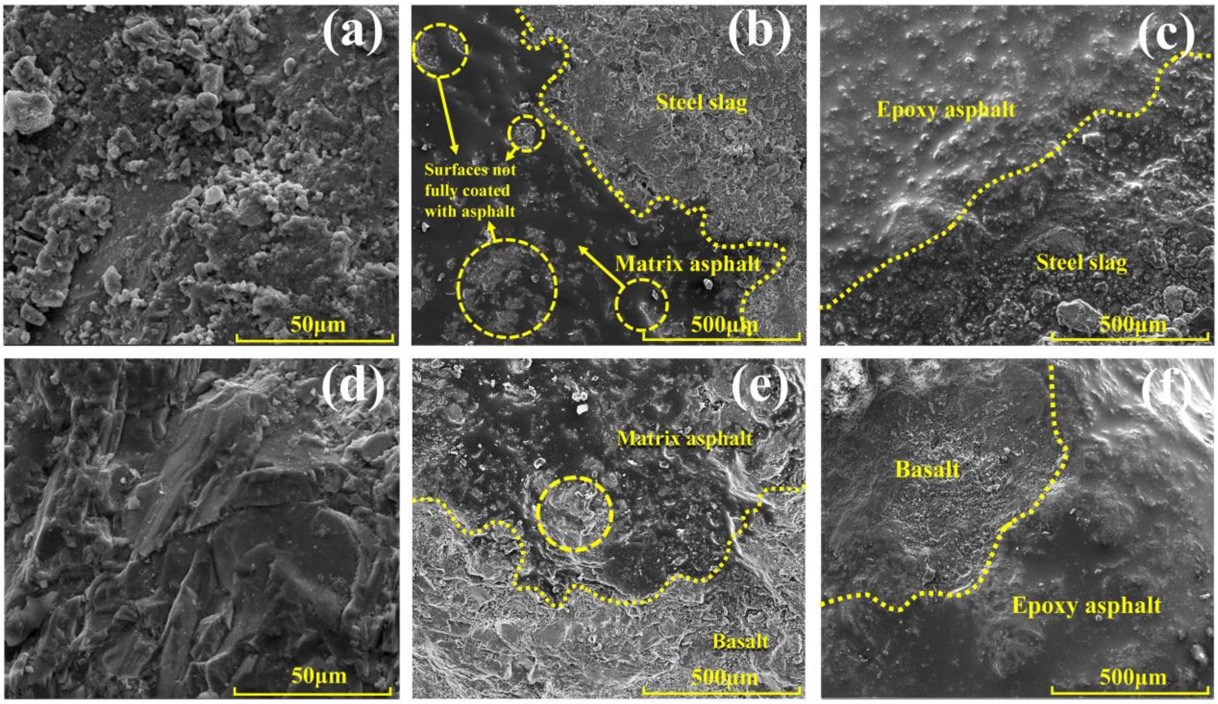

Fig. 10. Surface micromorphological results of SEM tests: (a) BA 5000×, (b) SS 5000×, (c) EA0-BA 300× (d) EA0-SS 300× (e) EA20 -BA 300×, (f) EA20-SS 300×

Based on the aforementioned macro- and micro-scale test results, Fig. 11 were employed to further elucidate the performance enhancement mechanism of EA in SSAM. Fig. 11(c) illustrates that as asphalt adhesion decreased, moisture gradually penetrated the interface between the matrix asphalt and SS. This penetration enabled a chemical reaction with free calcium oxide (*f*-CaO) on SS surfaces, forming $Ca(OH)_2$ and establishing a weak interlayer structure [20, 21], ultimately resulting in a significant reduction in adhesion at asphalt-aggregate interfaces. Under dynamic moisture conditions, this unstable interlayer promoted asphalt film delamination, adversely affecting volume stability and moisture damage resistance of asphalt mixtures [58, 59]. In contrast, microscopic tests confirmed that surface morphology and chemical composition of SS facilitated adhesion and mechanical anchoring with EA. As shown in Fig. 11(b) and (e), EA20 demonstrated superior adhesion compared to matrix asphalt, effectively coating SS surfaces. This significantly mitigated moisture-related deterioration at EA-SS interfaces, thereby improving the pavement performance of SSAM and providing theoretical support for the large-scale application of SS in pavement engineering.

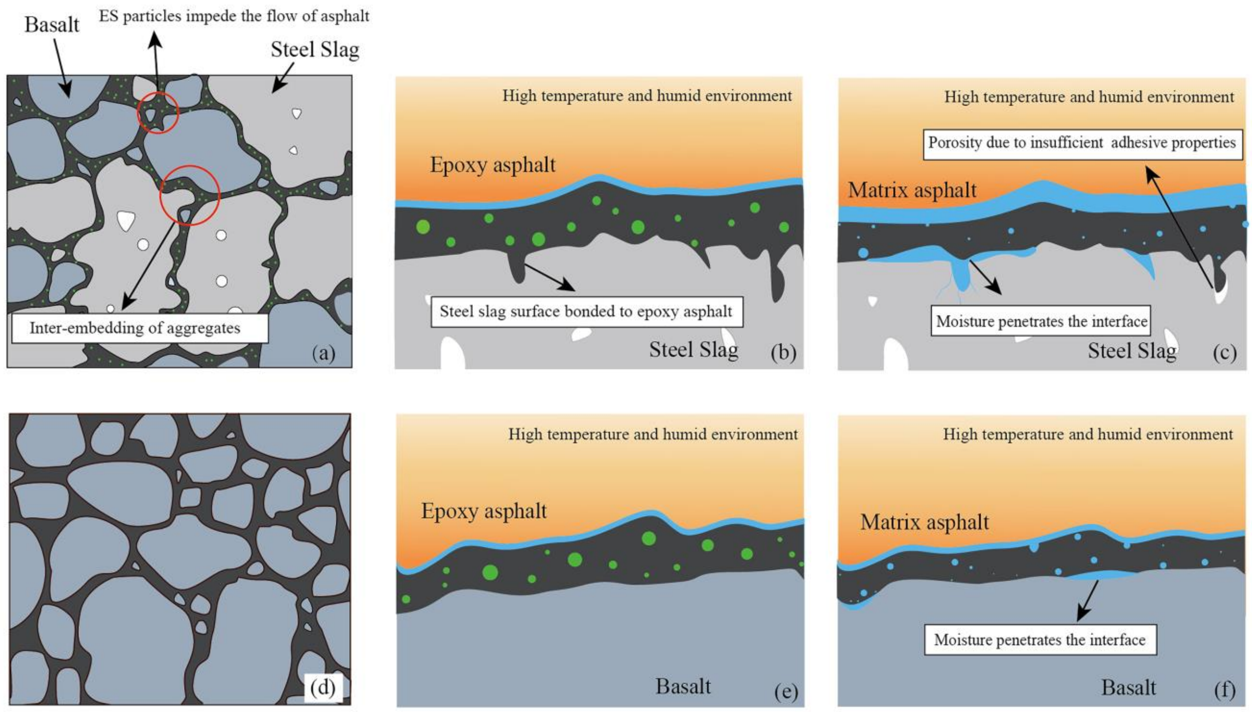

Fig. 11. Performance enhancement mechanism of EASSAM: (a) Structure of EA20SS100AM; (b) EASSAM in a high temperature and moisture environment; (c) EA0SSAM in a high temperature and moisture environment; (d) Structure of EA0SS0AM; (e) EA0SS0AM in a high temperature and moisture environment; (f) EA0SS0AM in a high temperature and moisture environment.

4.5. Economic and environmental benefits

To systematically evaluate the economic and environmental benefits of EA20SS100AM, this study selected a standard pavement section with a 5 cm surface layer thickness, 20 m width, and 100 m length as the analysis object. Calculations were performed for initial construction (including raw materials and construction phases), full life cycle (including raw materials, construction, maintenance, demolition, and recycling phases), as well as annualized costs and carbon emissions. Comparisons were made with commonly used SBS-modified asphalt mixture (SBSMAM). Referring to relevant literature and previous research results [60, 61], the costs and carbon emissions of raw materials are shown in Table 4. Additionally, energy consumption during the life cycle was determined according to the "Standards of Carbon Emission Calculation for Highway Construction" (T/CHSDA 0001-2024) [62]. Prior to calculations, the design service life of different mixtures needed to be determined. Fig. 12 presents the fatigue test results of SBSMAM and EA20SS100AM. At the 400 με strain level, EA20SS100AM exhibits an initial stiffness modulus of 24,887 MPa, which is 1.75 times that of SBSMAM. The N_f of SBSMAM and EA20SS100AM are 681,166 and 1,335,085 cycles respectively, with the latter being 1.96 times the former. It is noteworthy that pavements constructed with SBSMAM typically have a design service life of 15 years. However, relevant studies indicate that under the coupled effects of environmental factors and traffic loading, pavement performance generally undergoes significant deterioration after 8-10 years of service, necessitating surface rehabilitation or reconstruction [63, 64]. Therefore, this study set the design service life of SBSMAM at 8 years. In comparison, the superior fatigue performance of EA20SS100AM contributes to extending its service life. Assuming that the pavement structure, loading conditions, and environmental factors are the same for both mixtures, this study established the design service life of EA20SS100AM at 15 years. The calculated economic and environmental indicators are shown in Fig. 13.

Table 4. Cost and carbon emissions of raw materials

Material type	Cost/($/t)	Carbon emission/(kgCO$_2$e/t)
Matrix Asphalt	480.63	174.24
SBS modified asphalt	617.95	294.24
EA20	1,483.09	456.47
SS	6.87	2.82
Natural aggregate	41.20	5.84
Mineral powder	41.20	7.39

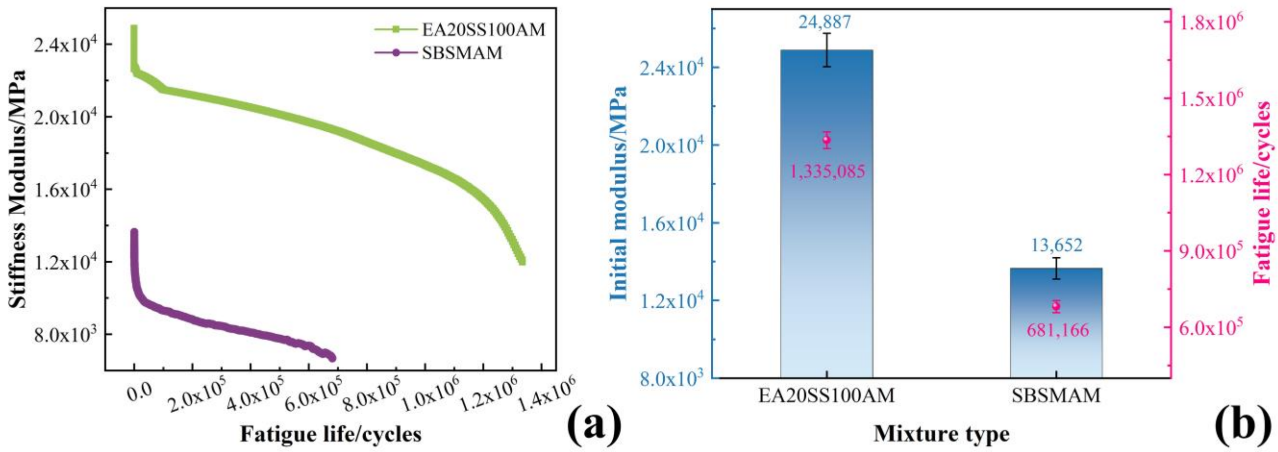

Fig. 12. Fatigue test results

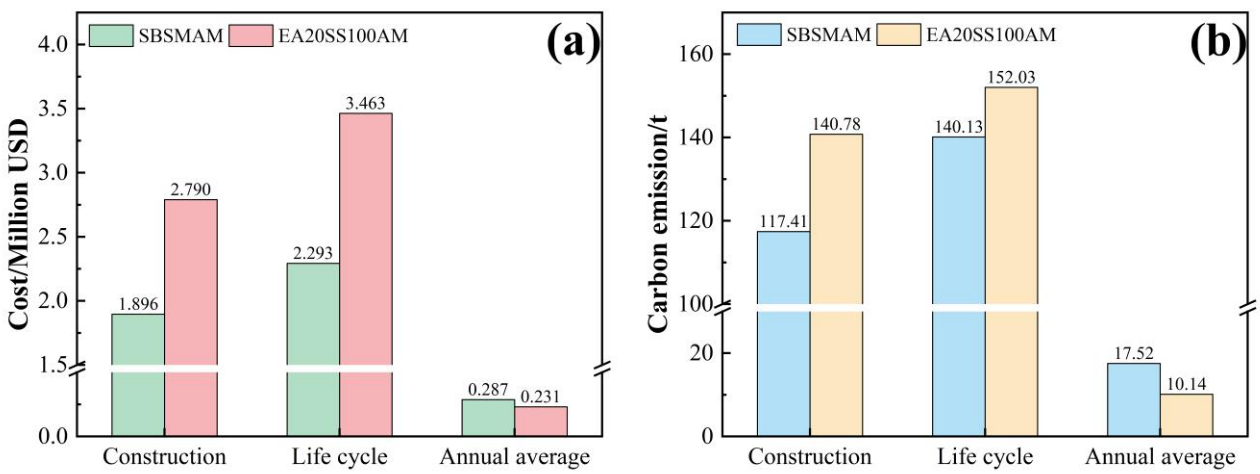

Fig. 13. Calculation of economic and environmental indicators for different pavements:

(a) cost; (b) carbon emissions

The cost analysis revealed that due to the high price of the ES system, the initial construction and full life-cycle costs of EA20SS100AM reached $2.790M and $3.463M respectively, both higher than those of SBSMAM. However, owing to its 15-year service life, the annual average cost of

EA20SS100AM amounted to $0.231M, representing a 19.5% reduction compared with SBSMAM. As shown in Fig. 11(b), similarly, the high carbon emissions from curing agents led to elevated carbon emissions for EA20, resulting in higher initial construction and full life-cycle carbon emissions for EA20SS100AM than SBSMAM. Notably, the annual average carbon emissions of EA20SS100AM measured 10.14 t, demonstrating a significant 42.1% decrease compared with the 17.52 t of SBSMAM. The results indicated that although EA20SS100AM required higher initial investment and generated higher carbon emissions, its outstanding durability translated into substantial life-cycle advantages, leading to remarkable reductions in both annualized cost and carbon emissions for pavements constructed with this material, thereby delivering significant economic and environmental benefits.

The leaching test results are presented in Table 5. In the SS leachate, all elements except arsenic (As) exceeded the standard limits specified in the Chinese standard "Environmental Quality Standards for Surface Water" (GB3838-2002) [65], indicating that large-scale stockpiling of SS would inevitably cause pollution to soil and groundwater. In contrast, the EA20SS100AM leachate showed Cd, Cr^{6+}, Hg, and As below detection limits (not detected), with only lead (Pb) being measurable at 0.0036 mg/L, but it was below the standard limit of ≤0.01 mg/L (GB3838-2002) [65]. Compared to previous asphalt mixtures prepared using pretreated SS under identical testing conditions, EA20SS100AM demonstrated significantly reduced heavy metal leaching [21]. These results further confirmed that EA could effectively encapsulate SS, preventing water infiltration and subsequent heavy metal leaching. Consequently, incorporating ES into SSAM not only enabled 100% replacement of natural coarse aggregates with SS and improved the overall pavement performance, but also achieved satisfactory economic and environmental benefits. This approach holds great significance for accelerating SS utilization, reducing natural mineral extraction, and promoting sustainable development in pavement engineering.

Table 5. Leaching test results

Material type	Element content/(mg/L)				
	Cd	Cr^{6+}	Pb	Hg	As
SS	0.0021	0.0162	0.1941	0.00042	0.0258
EA20SS100AM	ND	ND	0.0036	ND	ND
Limit of Detection	0.0004	0.0013	0.0003	0.00002	0.0001
Limit value (GB 3838-2002)	0.001	0.01	0.01	0.00005	0.05

5. Conclusions

This study introduced ES into SSAM and optimized the preparation process. The pavement performance of EASSAM with different ES contents and SS replacement ratios was analyzed, and microscopic tests were conducted to investigate the micro-scale improvement mechanisms. Additionally, an analysis of the economic and environmental benefits of EASSAM was performed. The main conclusions can be drawn as follows:

a) The application of ES not only eliminated the need for complex SS pretreatment but also significantly improved moisture stability, high-temperature stability, low-temperature cracking resistance, and long-term volume stability of SSAM. EA20SS100AM exhibited excellent comprehensive pavement performance, achieving 100% replacement of natural coarse aggregates with SS. Higher curing temperatures accelerated the curing process of EA, enabling faster traffic opening during summer construction.

b) ES dispersed uniformly in EA, enhancing adhesion between aggregates and asphalt. The high fluidity of EA20 enabled complete infiltration of the porous SS surface, forming dense coating layers and ensuring thorough filling of aggregate voids. This effectively inhibited moisture intrusion and SS expansion, significantly improving mixture durability.

c) While ES increased initial construction costs and carbon emissions of EASSAM, compared with SBSMAM, the outstanding durability of EA20SS100AM resulted in 19.5% and 42.1% reductions in annualized costs and carbon emissions respectively, demonstrating significant economic and environmental benefits. Meanwhile, the heavy metal leaching of EA20SS100AM was effectively suppressed. This holds great value for the large-scale application of SS in pavement engineering and promoting the green transformation of transportation infrastructure.

d) Future research should focus on transitioning EASSAM from laboratory studies to engineering applications and standardization. Optimization of ES formulations or adoption of more environmentally friendly bio-based epoxy materials could be considered to further reduce costs and environmental impacts.

Acknowledgements:

This work was undertaken with funding from the Major Science and Technology Project of Nanjing (No. 202209012), the Carbon Peak and Carbon Neutrality Science and Technology Innovation Special Funds of Jiangsu Province (No. BE2022615), the National Natural Science Foundation of China (No. 52278445), and the SEU Innovation Capability Enhancement Plan for Doctoral Students (No. CXJH_SEU 24041). Moreover, the author would like to express their gratitude to the China Scholarship Council (CSC) for funding this research.

Declaration of Interest statement

The authors declare that they have no known competing financial interests or personal relationships that could have appeared to influence the work reported in this paper.

References

[1] Y. Gu, W. Liu, B. Wang, B. Tian, X. Yang, C. Pan, Analysis and Prediction of Energy, Environmental and Economic Potentials in the Iron and Steel Industry of China, Processes 11(12) (2023) 3258.

[2] C. Li, L. Zhang, Q. Wang, D. Zhou, Towards low-carbon steel: System dynamics simulation of policies impact on green hydrogen steelmaking in China and the European Union, Energy Policy 188 (2024) 114073.

[3] J. Guo, Y. Bao, M. Wang, Steel slag in China: Treatment, recycling, and management, Waste management 78 (2018) 318-330.

[4] X. Yang, C. Zhang, X. Li, Z. Cao, P. Wang, H. Wang, G. Liu, Z. Xia, D. Zhu, W.-Q. Chen, Multinational dynamic steel cycle analysis reveals sequential decoupling between material use and economic growth, Ecological Economics 217 (2024) 108092.

[5] J. Sun, S. Luo, Y. Wang, Q. Dong, Z. Zhang, Pre-treatment of steel slag and its applicability in asphalt mixtures for sustainable pavements, Chemical Engineering Journal 476 (2023) 146802.

[6] W. Gao, W. Zhou, X. Lyu, X. Liu, H. Su, C. Li, H. Wang, Comprehensive utilization of steel slag: A review, Powder Technology 422 (2023) 118449.

[7] Y.N. Dhoble, S. Ahmed, Review on the innovative uses of steel slag for waste minimization, Journal of Material Cycles and Waste Management 20 (2018) 1373-1382.

[8] B. Xu, Y. Yi, Soft clay stabilization using ladle slag-ground granulated blastfurnace slag blend, Applied Clay Science 178 (2019) 105136.

[9] B. Xu, X.Y. Tan, Y. Yi, Synergistic approach for CO_2 capture and remediation of lead-contaminated soils utilizing steel slag, Journal of Environmental Chemical Engineering 13(5) (2025) 117543.

[10] L.P. Thives, E. Ghisi, Asphalt mixtures emission and energy consumption: A review, Renewable and Sustainable Energy Reviews 72 (2017) 473-484.

[11] D. Ioannidou, G. Meylan, G. Sonnemann, G. Habert, Is gravel becoming scarce? Evaluating the local criticality of construction aggregates, Resources, Conservation and Recycling 126 (2017) 25-33.

[12] Z. Chen, S. Wu, J. Wen, M. Zhao, M. Yi, J. Wan, Utilization of gneiss coarse aggregate and steel slag fine aggregate in asphalt mixture, Construction and Building Materials 93 (2015) 911-918.

[13] V.A. Nunes, P.H. Borges, Recent advances in the reuse of steel slags and future perspectives as binder and aggregate for alkali-activated materials, Construction and building materials 281 (2021) 122605.

[14] X. Zhao, Y. Sheng, H. Lv, H. Jia, Q. Liu, X. Ji, R. Xiong, J. Meng, Laboratory investigation on road performances of asphalt mixtures using steel slag and granite as aggregate, Construction and Building Materials 315 (2022) 125655.

[15] E.J. Lee, H.M. Park, Y.C. Suh, J.-S. Lee, Performance Evaluation of Asphalt Mixtures with 100% EAF and BOF Steel Slag Aggregates Using Laboratory Tests and Mechanistic Analyses, KSCE Journal of Civil Engineering 26(11) (2022) 4542-4551.

[16] A. Goli, The study of the feasibility of using recycled steel slag aggregate in hot mix asphalt, Case Studies in Construction Materials 16 (2022) e00861.

[17] Y. Sheng, R. Wang, H. Jia, W. Qiu, L. Feng, S. Zhang, S. Cui, X. Zhao, Study on the performance and adhesion behavior of ultrathin wearing course using calcined bauxite as aggregate, Mathematical Problems in Engineering 2021(1) (2021) 5535070.

[18] Z. Chen, Z. Gong, Y. Jiao, Y. Wang, K. Shi, J. Wu, Moisture stability improvement of asphalt mixture

considering the surface characteristics of steel slag coarse aggregate, Construction and Building Materials 251 (2020) 118987.

[19] Z. Ren, D. Li, Application of steel slag as an aggregate in concrete production: a review, Materials 16(17) (2023) 5841.

[20] Z. Chen, S. Wu, Y. Xiao, W. Zeng, M. Yi, J. Wan, Effect of hydration and silicone resin on Basic Oxygen Furnace slag and its asphalt mixture, Journal of Cleaner Production 112 (2016) 392-400.

[21] J. Sun, W. Huang, X. Wang, J. Hu, Y. Wang, Z. Zhang, S. Luo, Feasibility of pretreated steel slag for asphalt pavement application and risk assessment of hazardous substance leaching, Chemical Engineering Journal 498 (2024) 155497.

[22] M.R. Kakar, M.O. Hamzah, J. Valentin, A review on moisture damages of hot and warm mix asphalt and related investigations, Journal of Cleaner Production 99 (2015) 39-58.

[23] P. Cui, S. Wu, Y. Xiao, Q. Liu, F. Wang, Hazardous characteristics and variation in internal structure by hydrodynamic damage of BOF slag-based thin asphalt overlay, Journal of Hazardous Materials 412 (2021) 125344.

[24] S. Luo, J. Sun, J. Hu, S. Liu, Performance evolution mechanism of hot-mix epoxy asphalt binder and mixture based on component characteristics, Journal of Materials in Civil Engineering 34(9) (2022) 04022235.

[25] W. Jiang, D. Yuan, C. Xing, B. Zhang, J. Xiao, T. Wang, W. Wu, Experimental study of epoxy asphalt binder and porous epoxy asphalt concrete, Journal of Cleaner Production 420 (2023) 138373.

[26] K. Li, J. Xie, Y. Liu, Y. Tan, Y. Pan, Development and evaluation of roadway-oriented epoxy-modified asphalt binders and mixtures, Construction and Building Materials 418 (2024) 135398.

[27] Z. Qian, L. Chen, C. Jiang, S. Luo, Performance evaluation of a lightweight epoxy asphalt mixture for bascule bridge pavements, Construction and Building Materials 25(7) (2011) 3117-3122.

[28] S. Zhang, H. Zhang, M. Zhou, Investigation on the high-temperature stability and fatigue behavior of cold mixed epoxy asphalt mixture with different gradations, Case Studies in Construction Materials 20 (2024) e02694.

[29] M. Jia, A. Sha, J. Lin, Z. Zhang, B. Qi, D. Yuan, Polyurethane asphalt binder: A promising candidate for steel bridge deck-paving material, International Journal of Pavement Engineering 23(11) (2022) 3920-3929.

[30] J. Tian, S. Luo, Q. Lu, S. Liu, Effects of epoxy resin content on properties of hot mixing epoxy asphalt binders, Journal of Materials in Civil Engineering 34(7) (2022) 04022145.

[31] J. Sun, W. Huang, G. Lu, S. Luo, Y. Li, Investigation of the performance and micro-evolution mechanism of low-content thermosetting epoxy asphalt binder towards sustainable highway and bridge decks paving, Journal of Cleaner Production 384 (2023) 135588.

[32] R. Zhao, F. Jing, R. Wang, J. Cai, J. Zhang, Q. Wang, H. Xie, Influence of oligomer content on viscosity and dynamic mechanical properties of epoxy asphalt binders, Construction and Building Materials 338 (2022) 127524.

[33] Y. Fan, Y. Wu, H. Chen, S. Liu, W. Huang, H. Wang, J. Yang, Performance evaluation and structure optimization of low-emission mixed epoxy asphalt pavement, Materials 15(18) (2022) 6472.

[34] Ministry of Transport of China, Standard test methods of bitumen and bituminous mixtures for highway engineering, China Standard Press, Beijing, 2011.

[35] Standardization Administration of China, Plastics—Epoxy compounds—Determination of epoxy equivalent, China Standard Press, Beijing, 2008.

[36] State Administration of Market Supervision and Administration, Plastics - Determination of tensile properties, China Standard Press, Beijing, 2018.

[37] International Standards Organization, Plastics—Amine epoxide hardeners—Determination of primary, secondary and tertiary amine group nitrogen content, International Standards Organization, Switzerland, 1996.

[38] S. Dai, H. Zhu, M. Zhai, Q. Wu, Z. Yin, H. Qian, S. Hua, Stability of steel slag as fine aggregate and its application in 3D printing materials, Construction and Building Materials 299 (2021) 123938.

[39] Standardization Administration of China, Steel slag for road, China Standard Press, Beijing, 2009.

[40] Ministry of Transport of China, Test Methods of Aggregate for Highway Engineering, China Communications Press, Beijing, 2024.

[41] Z. Zhang, J. Sun, Z. Huang, F. Wang, M. Jia, W. Lv, J. Ye, A laboratory study of epoxy/polyurethane modified asphalt binders and mixtures suitable for flexible bridge deck pavement, Construction and Building Materials 274 (2021) 122084.

[42] J. Sun, S. Luo, W. Huang, Y. Li, Reducing epoxy resin content in a thermosetting epoxy asphalt mixture: A feasible method to facilitate application, Journal of Materials in Civil Engineering 35(10) (2023) 04023352.

[43] J. Sun, S. Luo, W. Huang, J. Hu, S. Liu, Structural optimization of steel bridge deck pavement based on mixture performance and mechanical simulation, Construction and Building Materials 367 (2023) 130217.

[44] J. Chen, J. Li, H. Wang, W. Huang, W. Sun, T. Xu, Preparation and effectiveness of composite phase change material for performance improvement of Open Graded Friction Course, Journal of Cleaner Production 214 (2019) 259-269.

[45] PRC environmental protection agency, Identification standards for hazardous wastes-Identification for extraction toxicity, China Environmental Science Press, Beijing, 2007.

[46] PRC environmental protection agency, Solid waste-Extraction procedure for leaching toxicity-Sulphuric acid & nitric acid method, China Environmental Science Press, Beijing, 2007.

[47] J.-S. Chen, S.-H. Wei, Engineering properties and performance of asphalt mixtures incorporating steel slag, Construction and Building Materials 128 (2016) 148-153.

[48] Ministry of Transport of China, Technical Specification for Construction of Highway Asphalt Pavements, China Communications Press, Beijing, 2004.

[49] Z. Zhou, Y. Shen, H. Zhang, Y. Wang, H. Yang, J. Pan, X. Wei, Sandstone-concrete interface debonding mechanism under freeze-thaw actions: fracture process and fracture criterion, Construction and Building Materials 294 (2021) 123526.

[50] J. Liu, J. Xu, Q. Liu, S. Wang, B. Yu, Steel slag for roadway construction: a review of material characteristics and application mechanisms, Journal of Materials in Civil Engineering 34(6) (2022) 03122001.

[51] M. Jia, Z. Zhang, N. Yang, B. Qi, W. Wang, Z. Huang, J. Sun, F. Luo, T. Huang, Performance evaluation of thermosetting and thermoplastic polyurethane asphalt mixtures, Journal of Materials in Civil Engineering 34(6) (2022) 04022097.

[52] Y. Gan, C. Li, W. Ke, Q. Deng, T. Yu, Study on pavement performance of steel slag asphalt mixture based on surface treatment, Case Studies in Construction Materials 16 (2022) e01131.

[53] P. Mohan, A critical review: the modification, properties, and applications of epoxy resins, Polymer-plastics technology and engineering 52(2) (2013) 107-125.

[54] F. Lohse, H. Zweifel, Photocrosslinking of epoxy resins, Epoxy resins and composites III, Springer2005, pp. 61-81.

[55] A. Yukimasa, One-Part Epoxy Resin, Three Bond Technical News 19(1) (1987) 1-10.

[56] H. Na, Y. Wang, X. Zhang, J. Li, Y. Zeng, P. Liu, Hydration activity and carbonation characteristics of dicalcium silicate in steel slag: A review, Metals 11(10) (2021) 1580.

[57] F. Wang, Y. Zhang, X. Song, L. Liu, X. Sun, P. Sun, Influence of Self-Emulsifying Waterborne Epoxy Resin with Novel Hardeners on Pore Structure and Permeability of Cement-Based Materials, Buildings 15(7) (2025) 997.

[58] Z. Dong, Z. Liu, P. Wang, T. Zhou, Modeling asphalt mastic modulus considering substrate–mastic interaction and adhesion, Construction and Building Materials 166 (2018) 324-333.

[59] Z. Dong, Z. Liu, C. Yang, X. Gong, Viscosity characterization of confined bitumen considering microaggregate-bitumen interactions, Computer-Aided Civil and Infrastructure Engineering 35(11) (2020) 1261-1275.

[60] X. Yi, Y.D. Wong, H. Chen, Y. Fan, J. Yang, W. Huang, Utilization of dry-method styrene-butadiene-styrene and epoxy polymer to enhance the aged asphalt binder: Properties evaluation and cost discussion, Journal of Cleaner Production 428 (2023) 139419.

[61] Z. Zhang, J. Sun, W. Huang, X. Zhang, G. Lu, S. Luo, Y. Wang, A dual-driven fusion model of evaluating the performance and carbon emissions for recycled waste pavement, Resources, Conservation and Recycling 212 (2025) 107895.

[62] China Highway Survey and Design Association, Standards of Carbon Emission Calculation for Highway Construction, China Highway Survey and Design Association, Beijing, 2024.

[63] J. Wang, M. Liu, Long-Term Mechanical Deterioration Trends and Mechanisms of SBS-Modified Asphalt Mixtures, Coatings 14(11) (2024) 1363.

[64] D. Zhang, Y. Zheng, G. Yuan, Y. Zhang, G. Qian, H. Zhang, Research on the field aging gradient behavior of SBS-modified bitumen at different depths of pavement by rheological and microscopic characterization, Fuel 329 (2022) 125192.

[65] PRC environmental protection agency, Environmental quality standards for surface water, China Environmental Science Press, Beijing, 2002.